New phase of superconducting NbN stabilized by heteroepitaxial film growth

Randolph E. Treece, Mike S. Osofsky, Earl F. Skelton, Syed B. Qadri, James S. Horwitz, and Douglas B. Chrisey
Naval Research Laboratory, Washington, D.C. 20375-5345

Thin films of a new, metastable phase of superconducting niobium nitride have been grown using pulsed laser deposition (PLD). This new NbN phase is stabilized by heteroepitaxial growth on (100) MgO and is shown to be a primitive cubic ($Pm3m$) distortion from the typical $B1$, or rocksalt structure. Structural and electrical characterization reveals that this NbN phase has a higher-superconducting critical temperature and a larger lattice parameter when compared with films of $B1$-NbN. Growth of this new phase demonstrates that PLD can be used as a synthesis tool to deposit new, metastable materials.

The next generation of microelectronic devices will be based on the discovery of new materials and the development of related processing technology. The traditional methods of synthesis and preparation, typically involving high temperatures and long reaction times, have been used to investigate a large number of combination of elements. These reactions usually occur near chemical equilibrium, producing the thermodynamically stable products. The materials of the future will require the production of *metastable* compounds, synthesized far from chemical equilibrium by new reaction methods.

Currently, high-powered lasers are being incorporated in a new physical vapor deposition technique called pulsed laser deposition (PLD).[1] PLD is being used in the development of new synthesis routes to the formation of metastable compounds so that their intrinsic properties can be accurately measured and evaluated for use in future applications. The deposition of thin films of metastable compounds, such as the infinite layer oxides $Ca_{1-x}Sr_xCuO_2$,[2] cubic boron nitride (c-BN),[3] carbon nitride (CN_x),[4] and amorphous $Ge_{1-x}C_x$,[5] using PLD has been reported.

In this paper, we report on the synthesis of a new phase of superconducting NbN by PLD and the structural and electrical characterization of this material. Niobium nitride is a refractory material with a bulk superconducting transition temperature (T_c) of ~16 K.[6] Thin films of NbN, typically deposited by sputtering methods,[7,8] also are being studied for applications in electronics. The low chemical reactivity, mechanical durability, high T_c $(T_c \gg 4.2$ K), and ease with which Josephson junctions can be reproducibly manufactured make NbN a good candidate for use in low-temperature digital electronics.[9] We have demonstrated that, depending on the pressure of the reactive gas atmosphere [N_2/H_2 (10%)], any one of several different NbN_x $(0 \leq x \leq 1.4)$ phases could be grown on 600 °C (100) MgO substrates by ablating niobium targets.[10,11] At deposition pressures between 1 and 20 mTorr, metallic Nb_2N was deposited, and at pressures greater than 100 mTorr, insulating Nb_3N_4 was grown. Superconducting NbN films were deposited at 60 mTorr. The NbN films grew in one of two different structures. One of these structures has never been reported. In this paper, we describe this new phase of NbN and compare it to the well-known NbN phase with the $B1$ structure.

The films were grown on heated (100) MgO by ablating Nb foil with a pulsed (10 Hz) excimer laser (248 nm) in a high-vacuum chamber backfilled with 60 mTorr of a reactive gas mixture [N_2/H_2 (10%)]. The details of film growth and characterization will be given elsewhere.[12] Film composition was determined by Rutherford backscattering spectroscopy (RBS) with 6.2 MeV He^{2+} ions. The error in nitrogen composition is $NbN_{1.0(\pm0.1)}$. While no oxygen was detected in the fits of the RBS spectra, the sensitivity of RBS to C, N, and O atoms is low relative to Nb. Oxygen levels up to $\sim5\%$ are undetectable by our current measurements, but at larger amounts, oxygen would be apparent in the RBS spectra. The NbN films also were examined by elastic recoil detection with 2.0 MeV He^{2+} and the amount of hydrogen incorporation was found to be $\sim3\%$. Structural characterization of the NbN films was accomplished using standard x-ray-diffraction (XRD) techniques. All films were measured on an automated diffractometer, equipped with a rotating anode x-ray generator. Cu $K\alpha$ radiation was selected with a graphite monochromator and 2θ scans were made in 0.02° steps, typically from 15° to 95°. High-temperature XRD was performed on a commercial high-temperature stage. Oscillation photographs also were recorded of several films to confirm their structural character. Temperature-dependent resistance [$R(T)$] measurements were performed by a standard ac four-point probe measurement.[11] J_c (4.2 K) was measured inductively as previously described.[13] Residual resistivity ratios (RRR) were measured between 300 and 20 K; RRR $= R$ (300 K)$/R$ (20 K). The critical temperatures (T_c) were characterized by two quantities: T_c $(R=0)$, the temperature, as determined from the $R(T)$ measurement, where $R=0$ (the value of the resistance equals the measurement noise), and T_{onset}, the temperature at which the superconducting transition begins.

The structure of the new phase was identified by XRD. The deposited films were single-crystal-like in orientation with the substrate and, therefore, only the $(h00)$ planes were visible in the XRD pattern.[14] The presence of a primitive cubic (PC) lattice, rather than the face-centered cubic lattice of the $B1$ structure, was first determined by the presence of (100) and (300) peaks in the diffractometer scan. An XRD pattern of the new phase is shown in Fig.
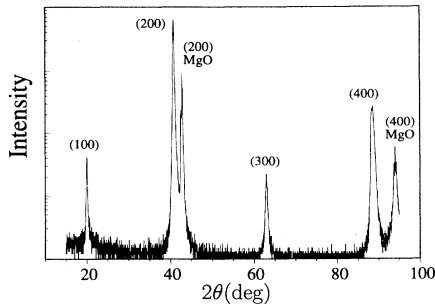
FIG. 1. XRD pattern of a superconducting NbN film adopting the new primitive cubic structure. The Miller indices are labeled. Note that the (100) and (300) reflections are forbidden in a fcc lattice.

1. All the $(h00)$ peaks expected of the $B1$ structure of NbN,[15] including those of the primitive cubic lattice forbidden by the $Fm3m$ symmetry, within the range of measurement were seen.

The observation of the PC lattice was confirmed in an oscillation photograph. Figure 2 shows an oscillation photograph taken of a film whose XRD pattern showed the new phase. Two sets of diffraction spots are present and indexed,[16] one set from the single-crystal MgO substrate (Miller indices underlined) and the other set from the deposited NbN film (Miller indices not underlined). The presence of spots for the NbN, instead of arcs or rings, indicates that it is epitaxially oriented in the ab plane, as well as in the c direction. Each substrate spot also is associated with a film diffraction spot. The difference between the fcc lattice of the substrate and the PC lattice of the film is evidenced by the additional spots corresponding to the (300) reflection in the zero layer, the (411) reflection in the first layer, and the $(12\bar{2})$ reflection in the second layer, as indicated on the photograph. The lattice parameter of the PC-NbN film was calculated based on the oscillation photograph. By plotting $(h^2+k^2+l^2)^{1/2}$ versus l/d (Å), a was found to be 4.442(2) Å.[11] We further confirmed the PC lattice by using the orientation matrix to locate and measure the (411) reflection on the diffractometer.[11]

Since the films were only ~ 1000 Å thick, we were not able to collect a full set of x-ray intensity data. However, our measured intensities for the $(h00)$ peaks $(h=1,2,\ldots,5)$ are consistent with our calculated intensities assuming the structure of the new phase of NbN is isomorphic with the primitive cubic structure of NbO, viz., space group $Pm3m$ with the Nb and N atoms in positions $3(c)$ and $3(d)$, respectively.[17] This latter structure can be derived from the $B1$ structure by removing the Nb and N atoms located at $(0,0,0)$ and $(\frac{1}{2},\frac{1}{2},\frac{1}{2})$, respectively.

The PC-NbN phase could be stabilized only over a narrow range of substrate deposition temperatures, T_{sub}. The cubic lattice parameters of the deposited films were sensitive to T_{sub} and correlated with the NbN structural phase, as shown in Fig. 3. The film grown at room temperature (open triangle) was polycrystalline with a $B1$ structure and $a=4.378(5)$ Å. The films grown at 150, 700, 800, and 900 °C (closed squares) were highly $(h00)$ oriented in the $B1$ phase with 4.408 Å$\leq a \leq 4.420$ Å. When the substrate temperature was between 400 and 650 °C (open squares), the deposited films adopted the PC
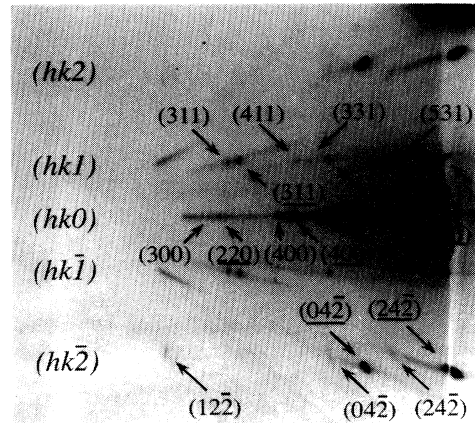

FIG. 2. Oscillation photograph of the primitive cubic phase of NbN deposited on (100) MgO with identification of the zeroth, first, and second diffraction layers. The Miller indices of the MgO substrate are underlined while those of the PC-NbN film are not. Note the (300), (411), and $(12\bar{2})$ diffraction spots of the NbN film characteristic of the primitive cubic phase.

lattice and displayed 4.438 Å$\leq a \leq 4.442$ Å. This is consistent with what was observed with the oscillation photograph.

Growth of the metastable phase also required deposition on an oriented substrate. When NbN films were deposited simultaneously on (100)MgO and amorphous SiO_2 at 600 °C, the metastable phase only would grow on the MgO substrate.[18] The film deposited on the fused silica was polycrystalline $B1$-NbN.

The metastability of the primitive cubic phase is reflected in the temperature dependence of the Bragg
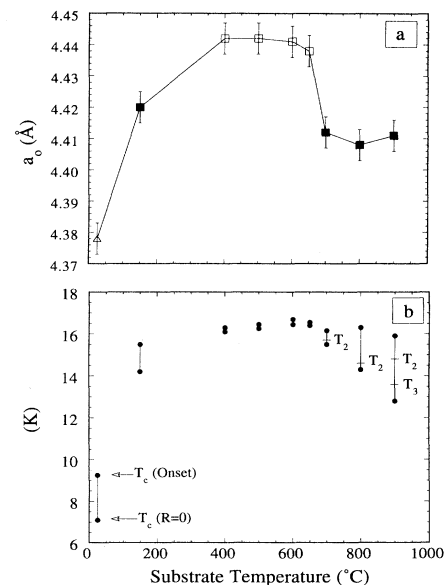

FIG. 3. (a) Lattice parameters of the deposited films are plotted as a function of substrate temperature. The films identified with the open triangle, closed squares, and open squares grew as polycrystalline $B1$, as oriented $B1$, and as heteroepitaxial primitive cubic, respectively. (b) T_{onset} and T_c $(R=0)$ for each deposited film are plotted as a function of substrate deposition temperature. T_2 and T_3 signify second and third transition onsets.

peaks. XRD measurements on a PC-NbN film were performed on a commercial high-temperature stage. As the temperature of the sample was increased from 400 to 600 °C, a precipitous decrease was observed in the intensity of the odd-order (h00) reflections. This decrease was significantly greater than that expected from the Debye-Waller factor. To quantify this, we compared the measured and calculated intensity ratios of the (100) peak at 400 °C and at 600 °C. The measured decrease was about 10:1. To estimate the size of the decrease expected from the increased thermal vibrations, $\langle u^2(T) \rangle$, we extrapolated measured mean-square atomic displacements for Nb and C and assumed that values for $\langle u_C^2(T) \rangle$ could be substituted for $\langle u_N^2(T) \rangle$.[19] Our computed estimate for this ratio is only 1%, an order of magnitude smaller than what is measured. An obvious explanation is that at elevated temperatures the metastable PC phase converts back to the $B1$ structure.

The PC-NbN displayed sharp superconducting transitions and high critical currents. The onset of superconductivity (T_{onset}) and T_c ($R = 0$) are plotted as a function of substrate deposition temperature [Fig. 3(b)]. Except for the lowest deposition temperature, T_{onset} is fairly independent of substrate temperature. On the other hand, T_c ($R = 0$) is quite sensitive to the deposition temperature. T_c ($R = 0$) increases sharply as deposition temperature is raised from 25 to 400 °C, producing very sharp transitions (~ 0.1 K) which remain relatively unchanged from 400 to 650 °C. The highest critical temperature measured was T_c ($R = 0$) $= 16.4$ K, measured for the film deposited at 600 °C. As the deposition temperature is raised from 650 to 900 °C, the transitions broaden and second and third T_{onset}'s appear. The critical current (J_c) measured by inductive methods for a PC-NbN film was 7.1 MA/cm^2.

The RRR's were sensitive to the deposition temperature, while the room-temperature (RT) resistivities, except for the sample grown at $T_{sub} = 25$ °C, were not. A plot of RT resistivity and RRR versus deposition temperature is shown in Fig. 4. The RT resistivities of films deposited at 25 °C were > 300 $\mu\Omega$ cm. Raising the deposition temperature to 150 °C and above resulted in lowering the resistivity to < 100 $\mu\Omega$ cm. The lowest RT resistivity observed was 52 $\mu\Omega$ cm for a film grown at 650 °C. RRR's increased from 0.3 to 1.3 as T_{sub} was raised from 25 to 400 °C. The PC-NbN films grown at temperatures between 400 to 650 °C displayed metallic character in $R(T)$ measurements. For films grown at temperatures > 650 °C, the RRR was < 1 and decreased as T_{sub} was raised from 700 to 900 °C.

RBS spectra showed that the films grown at temperatures of 150 °C and above had the same compositions, within experimental error, with ratios of nitrogen to niobium of $1.0 \leq$ N/Nb ≤ 1.1. The film grown at RT had considerably more nitrogen present with N/Nb$=1.4$. There were neither oxygen nor carbon detected by RBS in the deposited films.

Other than the samples grown at room temperature (and possibly 150 °C), whose properties are due largely to the poor crystallinity of the film, this study has revealed trends in several physical characteristics which prove the
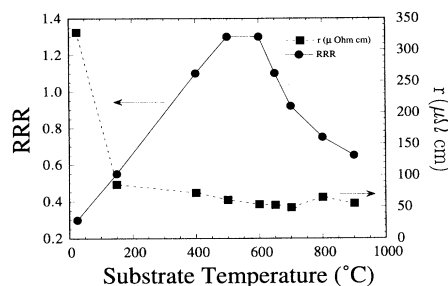

FIG. 4. A plot of RT resistivity and RRR as a function of deposition temperature.

existence of a new, metastable phase of NbN. These trends are a result of the rich Nb-N phase diagram and reflect the interplay of properties between superconducting phases of NbN (including the new one) and insulating phases, possibly Nb_3N_4.[9] Films deposited between 400 and 650 °C are single-phase NbN adopting the new structure. This new phase is manifested by a change in structure and transport properties from samples grown at T_{sub} below 400 °C and above 650 °C, and could not be stabilized on an amorphous substrate.

The properties that correlate with the structural phase transition are the unit-cell symmetry, a, RRR, and transition width. When compared to the NbN films grown by PLD with the $B1$ structure, the films deposited at 400 °C $\leq T_{sub} \leq 650$ °C displayed several key differences. The differences include a new unit cell (primitive cubic), larger lattice parameters (by about 7%), larger RRR values (> 1), narrower transition widths (~ 0.1 K), and a single superconducting transition. With all of these differences, the room-temperature resistivity and the spatially averaged N/Nb ratio ($1.0 \leq$ N/Nb ≤ 1.1) remain relatively constant as T_{sub} is increased from 150 to 900 °C.

The metastable NbN phase has a lattice parameter considerably larger than that of $B1$-NbN and is stabilized by epitaxial growth. Previous reports of $a \approx 4.44$ Å for NbN films involved films which actually contained significant amounts of carbon and could be described as NbN_xC_{1-x}.[6,20] While there have been reports of epitaxial NbN films, this is the first report of the PC-phase of NbN. Previously, sputtering and vapor-phase techniques have been used to grow NbN epitaxially on (100) MgO at similar substrate deposition temperatures,[21,22] but these films adopted the well-known $B1$ structure.

The evolution of the structural and electrical properties of PLD films as a function of T_{sub} can be explained phenomenologically by a granular superconductor model in which the samples consist of grains of superconducting phases of NbN with different T_c's surrounded by an insulating phase, Nb_3N_4. In this model, films deposited at substrate temperatures between 400 and 650 °C consist of single-phase (i.e., little, or no, insulating grain boundaries) metallic NbN which is distorted by excess N and stabilized by the oriented substrate thus creating the new phase with $T_c > 16.4$ K and a larger than normal lattice parameter. Films made at the higher and lower substrate temperatures consist of several phases: (1) small amounts of the new material (thus maintaining the $T_{onset} > 16$ K);

(2) a majority of undistorted B1-NbN phase(s) with lower T_c('s) and the conventional lattice parameter; and (3) small amounts of insulating Nb_3N_4 which forms a thin shell around the superconducting grains.

The variation in thickness of this thin shell of insulating phase accounts for all of the observations: constant room-temperature resistivity and constant average N/Nb across the range of deposition temperatures, while a, RRR, and transitions vary. The resistivity behavior can be explained using the granular model in which the sample resistance is composed of a sum of intragranular, intrinsic metallic resistance and insulating intergranular resistance (due to the Nb_3N_4 shell). The contribution of thin shells to the total room-temperature resistance would be small, consistent with our results, and would increase as the temperature decreased, producing a slight activation in the samples' $R(T)$ behavior (again consistent with our observations). As the shell thickens with increased deposition temperature, the $R(T)$ becomes more activated, i.e., the RRR decreases, as is observed. The formation of Nb_3N_4 requires that the excess N precipitates out of the interior of the primitive cubic NbN grains leaving the conventional material with the commonly observed a, but allowing the average N/Nb ratio to remain the same.

The final question to be addressed is why there are multiple T_c's while the room-temperature resistivity and, hence, the nature of the conduction band remains unchanged. The relationship between T_c and material parameters is described by the solution to the Eliashberg equation:[23]

$$T_c = 0.25 \langle \Omega^2 \rangle^{1/2} / [e^{2/\lambda_{\text{eff}}} - 1]^{1/2} , \qquad (1)$$

where $\langle \Omega^2 \rangle^{1/2}$ is a weighted average phonon frequency and λ_{eff} is the effective electron-phonon coupling strength which is a function of $\langle \Omega^2 \rangle^{1/2}$. From this equation it is clear that T_c will change if the phonon spectrum is altered. Since phonon spectra are dependent on crystallographic structure, changes in NbN structure should affect $\langle \Omega^2 \rangle^{1/2}$, leading to different T_c's for each phase.

The deposition of the new material by PLD may be due to the unique aspects of this growth technique, since previous epitaxial NbN films on (100) MgO grew in the B1 structure. PLD is different from equilibrium growth techniques in several ways. In PLD, the depositing vapor arrives in short pulses which are separated by relatively long reorganization times on the surface between pulses. Although the average deposition rates between PLD and equilibrium techniques are comparable, the instantaneous growth rate during the pulsed arrival can be as high as 10^5 Å/sec. In addition, the laser-generated plasma contains ions and neutral particles with high (≤ 100 eV) kinetic energies. For oxides, these high kinetic energies have been shown to increase gas phase reaction cross sections.

In conclusion, we have synthesized a new, metastable phase of NbN by PLD. The new phase is a primitive cubic distortion from the well-known B1 structure. The electronic transport properties (as measured by T_c, transition width J_c, and RT resistivity) of the PC-NbN are equivalent to, or exceed those of the B1 material. The metastable PC phase is stabilized on (100) MgO and can be transformed back to the B1 phase by reheating the samples. The discovery of the new phase in films grown by PLD suggests that stabilization of the metastable material may require the growth dynamics particular to this method.

[1] Broader discussions of PLD are reviewed in *Pulsed Laser Deposition of Thin Films,* edited by D. B. Chrisey and G. K. Hubler (Wiley, New York, 1994); J. T. Cheung and H. Sankur, CRC Crit. Rev. Solid State Mater. Sci. **15**, 63 (1988).

[2] C. Niu and C. M. Lieber, J. Am. Chem. Soc. **114**, 3570 (1992); D. P. Norton *et al.* Appl. Phys. Lett. **62**, 1679 (1993).

[3] A. K. Ballal *et al.*, Mater. Res. Soc. Proc. **285**, 513 (1993); A. K. Ballal *et al.*, Thin Solid Films, **224**, 46 (1993); F. Qian *et al.*, Appl. Phys. Lett. **63**, 317 (1993).

[4] R. E. Treece *et al.*, Mater. Res. Soc. Proc. **327**, 243 (1994); F. Xiong and R. P. H. Chang, *ibid.* **285**, 587 (1993); C. Niu *et al.*, Science **261**, 334 (1993).

[5] H. Yuan and R. S. Williams, Chem. Mater. **5**, 479 (1993).

[6] L. E. Toth, in *Transition Metal Carbides and Nitrides,* edited by J. L. Margrave (Academic, New York, 1971), Vol. 7.

[7] S. A. Wolf *et al.*, J. Vac. Sci. Technol. **18**, 253 (1981); E. J. Cukauskas *et al.*, J. Appl. Phys. **57**, 2538 (1985).

[8] A. Shoji *et al.*, Appl. Phys. Lett. **60**, 1624 (1992).

[9] *Superconducting Electronics,* edited by H. Weinstock and M. Nisenoff (Springer-Verlag, New York, 1992).

[10] R. E. Treece, J. S. Horwitz, D. B. Chrisey, and E. P. Donovan, Chem. Mater. **6**, 2205 (1994).

[11] R. E. Treece *et al.*, Mater. Res. Soc. Proc. **343**, 747 (1994).

[12] R. E. Treece, M. Osofsky, E. Skelton, S. Qadri, J. S. Horwitz, and D. B. Chrisey (unpublished).

[13] J. H. Claassen *et al.*, Rev. Sci. Instrum. **62**, 996 (1991).

[14] The $[h00]$-reciprocal lattice vector of the NbN is normal to the largest face of the substrate and the sample was mounted on the diffractometer such that the $(h00)$ reflections would be observed at $\chi \sim 0°$.

[15] Powder Diffraction File (Joint Committee on Powder Diffraction Standards-International Center for Diffraction Data, Swarthmore, PA, 1986), File No. 38-1155 (NbN).

[16] Only the $(hk0)$, the $(hk\bar{2})$, and the $(hk1)$ layers are labeled because the $(hk2)$ and the $(hk\bar{1})$ are related by symmetry.

[17] A. L. Bowman *et al.*, Acta Crystallogr. **21**, 843 (1966).

[18] R. E. Treece *et al.*, Appl. Phys. Lett. **65**, 2860 (1994).

[19] E. F. Skelton, Acta Crystallogr. **A32**, 467 (1976).

[20] S. B. Qadri *et al.*, J. Vac. Sci. Technol. A **3**, 664 (1985); D. D. Bacon *et al.*, J. Appl. Phys. **54**, 6509 (1983).

[21] G. Oya and Y. Onodera, J. Appl. Phys. **45**, 1389 (1974); D. A. Rudman *et al.*, IEEE Trans. Mag. **MAG-23**, 831 (1987).

[22] T. L. Francavilla *et al.*, Jpn. J. Appl. Phys. **26**, Suppl. 26-3, 951 (1987); J. Talvacchio and A. I. Braginski, IEEE Trans. Mag. **MAG-23**, 859 (1987).

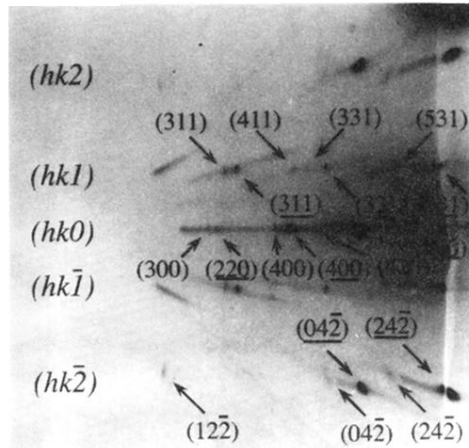[23] V. Z. Kresin, Phys. Lett. A **122**, 434 (1987).

FIG. 2. Oscillation photograph of the primitive cubic phase of NbN deposited on (100) MgO with identification of the zeroth, first, and second diffraction layers. The Miller indices of the MgO substrate are underlined while those of the PC-NbN film are not. Note the (300), (411), and (12$\bar{2}$) diffraction spots of the NbN film characteristic of the primitive cubic phase.